Supplementary Information

Highly efficient and stable plastic upcycling via metal encapsulation in zeolites

Tian Tan[1,7], Wangyang Wang[1,7], Liang Bai[1,7], Fanfei Sun[2,7], Qinghong Zhang[1], Xiao Chen[3], Yi-chi Wang[4], Yuhao Wang[5], Xiaofeng Xu[2], Wei Zhou[6], Colin Hansen[6], Tai-Ping Zhou[1], Xuejiao Wu[1], Haiwei Lai[1], Jiyang Xie[1], Jincan Kang[1], Lei Zeng[1], Biao Zhang[1], Kang Cheng[1], Binju Wang[1], Weiping Deng[1]*, Christophe Copéret[6]*, Gang Fu[1]*, Ye Wang[1]*

[1]State Key Laboratory of Physical Chemistry of Solid Surfaces, Innovation Laboratory for Sciences and Technologies of Energy Materials of Fujian Province (IKKEM), National Engineering Laboratory for Green Chemical Productions of Alcohols, Ethers and Esters, College of Chemistry and Chemical Engineering, Xiamen University, Xiamen 361005, China

[2]Shanghai Synchrotron Radiation Facility, Shanghai Advanced Research Institute, Chinese Academy of Sciences, Shanghai 201204, China

[3]Beijing National Center for Electron Microscopy and Laboratory of Advanced Materials, School of Materials Science and Engineering, Tsinghua University, Beijing 100084, China

[4]Department of Chemical Engineering, Tsinghua University, Beijing, 100084, China

[5]Faculty of Metallurgical and Energy Engineering, Kunming University of Science and Technology, Kunming 650093, China

[6]Department of Chemistry and Applied Biosciences, ETH Zürich, CH-8093 Zürich, Switzerland

[7]Authors contributed equally: Tian Tan, Wangyang Wang, Liang Bai, Fanfei Sun

Corresponding authors: dengwp@xmu.edu.cn (Weiping Deng), ccoperet@inorg.chem.ethz.ch (Christophe Copéret), gfu@xmu.edu.cn (Gang Fu), wangye@xmu.edu.cn (Ye Wang)

This file includes:

Supplementary methods for the quantification of products

Supplementary Figures 1 to 11

Supplementary Tables 1 to 6

5

Supplementary methods for the quantification of products

For Gaseous products:

From TCD

$$n_{\mathrm{CH_4}} = k_1 \times \frac{n_{\mathrm{Ar}}}{S_{\mathrm{Ar}}} \times S_{\mathrm{CH_4}} \quad (1)$$

where n_{CH4} and n_{Ar} represent the moles of CH_4 and Ar, respectively. k_1 is the CH_4-Ar correction factor. S_{CH4} and S_{Ar} denote the integrated peak areas of CH_4 and Ar on the TCD, respectively.

From FID

$$n_i = \frac{n_{\mathrm{CH_4}}}{i \times S_{\mathrm{CH_4}}} \times S_i \quad (2)$$

where n_i and n_{CH4} represent the moles of gas product i (i = carbon number) and CH_4, respectively. S_i and S_{CH4} denote the integrated peak areas of gas product i (i = carbon number) and CH_4 on the FID, respectively.

$$n_{\mathrm{gas}} = \sum_{i=1}^{8} i \times n_i \quad (3)$$

where n_{gas} is the moles of total carbon atoms in gaseous products.

For Liquid products:

$$n_i = k_2 \times \frac{9 \times n_{\mathrm{C_9H_{12}}}}{i \times S_{\mathrm{C_9H_{12}}}} \times S_i \quad (4)$$

where n_i and n_{C9H12} represent the moles of liquid product i (i = carbon number) and C_9H_{12} (the internal standard), respectively. k_2 is the C_9H_{12}/n-C_9H_{20} correction factor. S_i denotes the integrated peak area of liquid product i (i = carbon number) on the FID.

$$n_{liquid} = \sum_{i=4}^{12} i \times n_i \quad (5)$$

where n_{liquid} denotes the mole of total carbon atoms in liquid product. n_i represents the mole of liquid product i (i = carbon number).

$$\text{Yield}\ (\%) = \frac{\sum_{i=1}^{8} i*n_i(\text{gas}) + \sum_{i=4}^{12} i*n_i(\text{liquid})}{m_{\mathrm{LDPE}}/14} \times 100\% \quad (6)$$

where n_i(gas) and n_i(liquid) represent the moles of product i (i = carbon number) in gas and liquid phases, respectively. m_{LDPE} denotes the mass of LDPE.

$$C_i \text{ selectivity } (\%) = \frac{n_i(\mathrm{gas}) + n_i(\mathrm{liquild})}{n_{\mathrm{gas}} + n_{\mathrm{liquild}}} \times 100\% \quad (7)$$

where C_i selectivity is the selectivity of product i (i = carbon number). n_i(gas) and n_i(liquid) are the moles of product i in gas and liquid phases, respectively. n_{gas} and n_{liquid} are the moles of total carbon atoms in gaseous and liquid products, respectively.

The insoluble solid residues including the catalyst and insoluble hydrocarbons, were dried at 100 ºC for 2 hours and then weighed. The mass of insoluble hydrocarbons was obtained by subtracting the mass of the catalyst from the total residue mass, and the conversion was calculated as follows:

$$\text{Conversion } (\%) = \frac{m_{\mathrm{residue}} - m_{\mathrm{catalyst}}}{m_{\mathrm{LDPE}}} \times 100\% \quad (8)$$

where m_{residue} and m_{catalyst} are the masses of the solid residue after the reaction and the catalyst, respectively; m_{LDPE} is the mass of LDPE before the reaction.

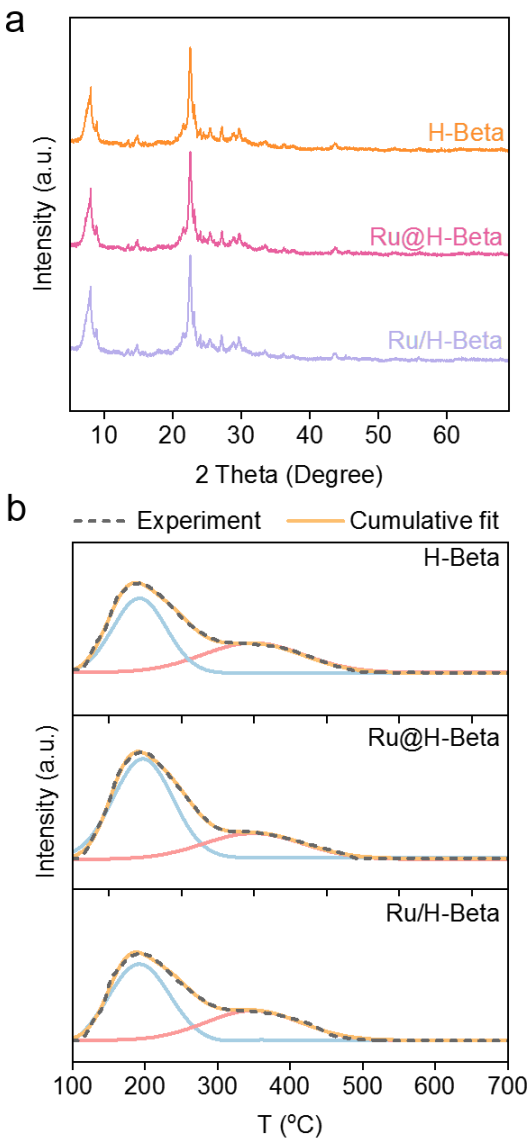

Supplementary Fig. 1. Characterizations of H-Beta, Ru@H-Beta, and Ru/H-Beta. (a) XRD patterns. (b) NH_3-TPD.

Quantification of Brønsted acid density was conducted by integrating the fitted peak ascribed to the Brønsted acid (desorption peak at around 350 ºC)[61], and the result was displayed in Supplementary Table 1.

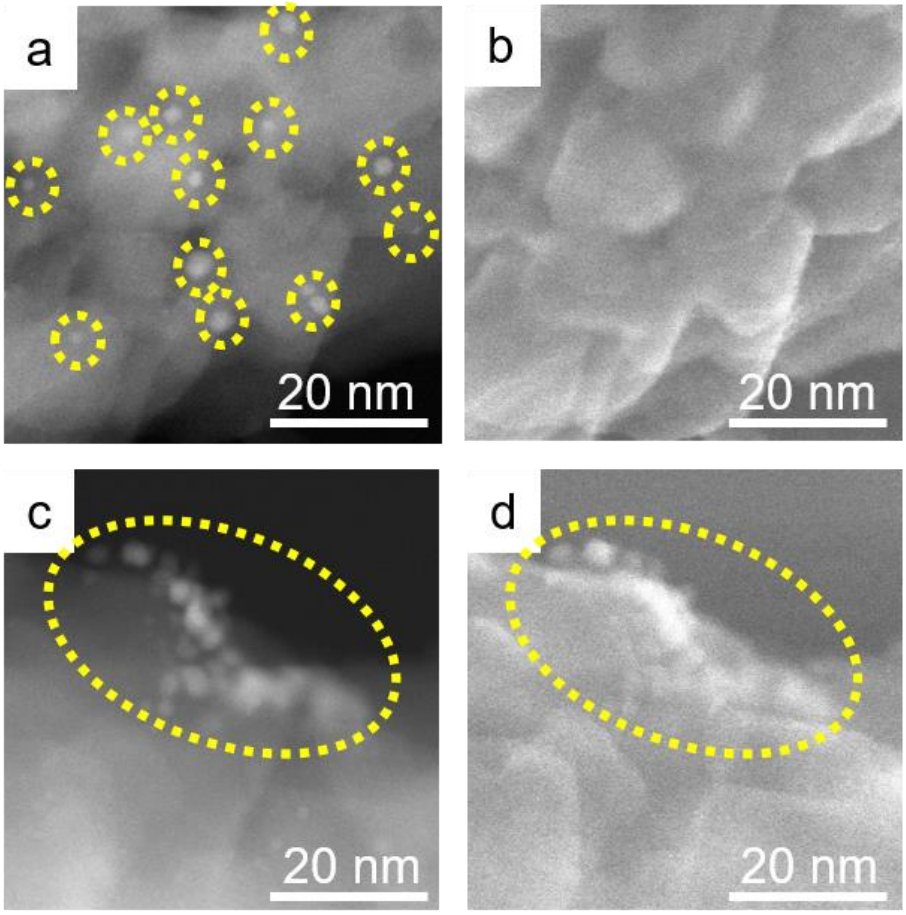

Supplementary Fig. 2. TEM micrographs. (a,b) Ru@H-Beta. (c,d) Ru/H-Beta. (a,c) Dark-field TEM. (b,d) secondary-electron TEM (SE-TEM).

SE-TEM, a surface-sensitive technique, was used together with TEM to distinguish the surface particles. The bright spots circled in (a) are Ru nanoparticles in Ru@H-Beta, which disappear in (b), indicating that these particles are not on the external surfaces of H-Beta. In contrast, Ru nanoparticles in Ru/H-Beta are observed in both (c) and (d), revealing that these Ru particles are located on the external surfaces of H-Beta.

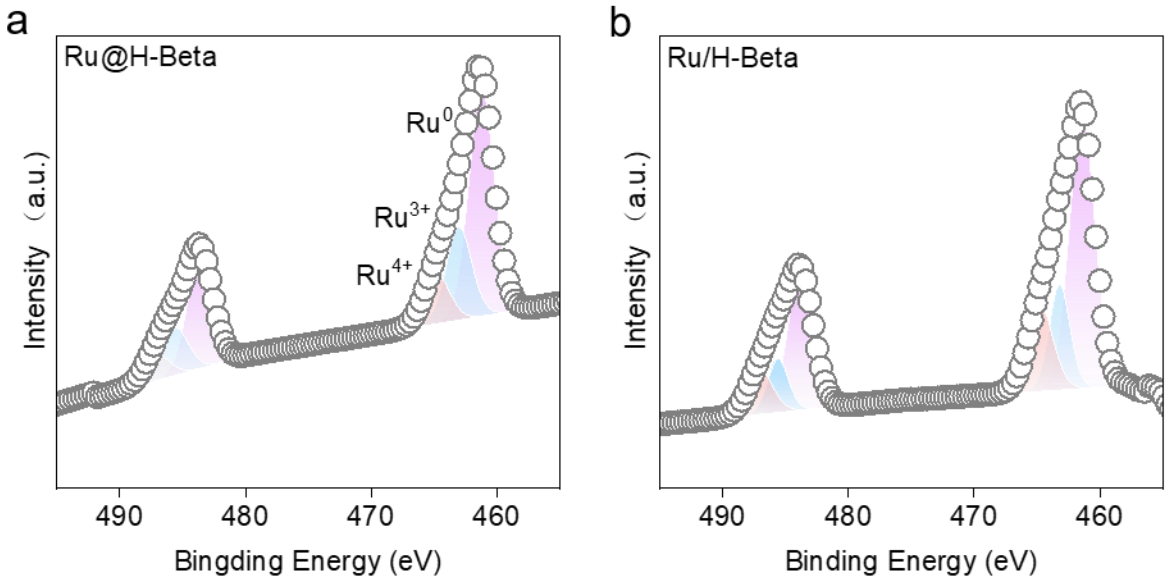

Supplementary Fig. 3. Ru 3d XPS spectra. (a) Ru@H-Beta. (b) Ru/H-Beta.

Ru@H-Beta was Ar^+-sputtered to ~10 nm to gain information about the Ru nanoparticles encapsulated inside zeolite crystals. Deconvolution shows that both catalysts contain virtually the same Ru species, with metallic Ru (Ru^0) as the dominant component.

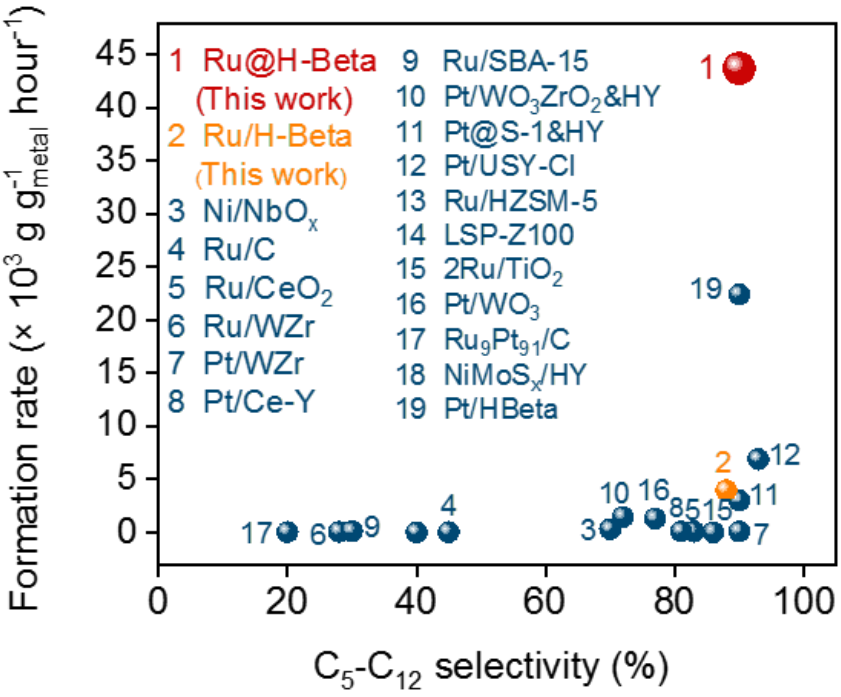

Supplementary Fig. 4. C_5–C_{12} formation rates on metal basis over various catalysts. Detailed catalytic performances, reaction conditions, and related references are listed in Supplementary Table 3.

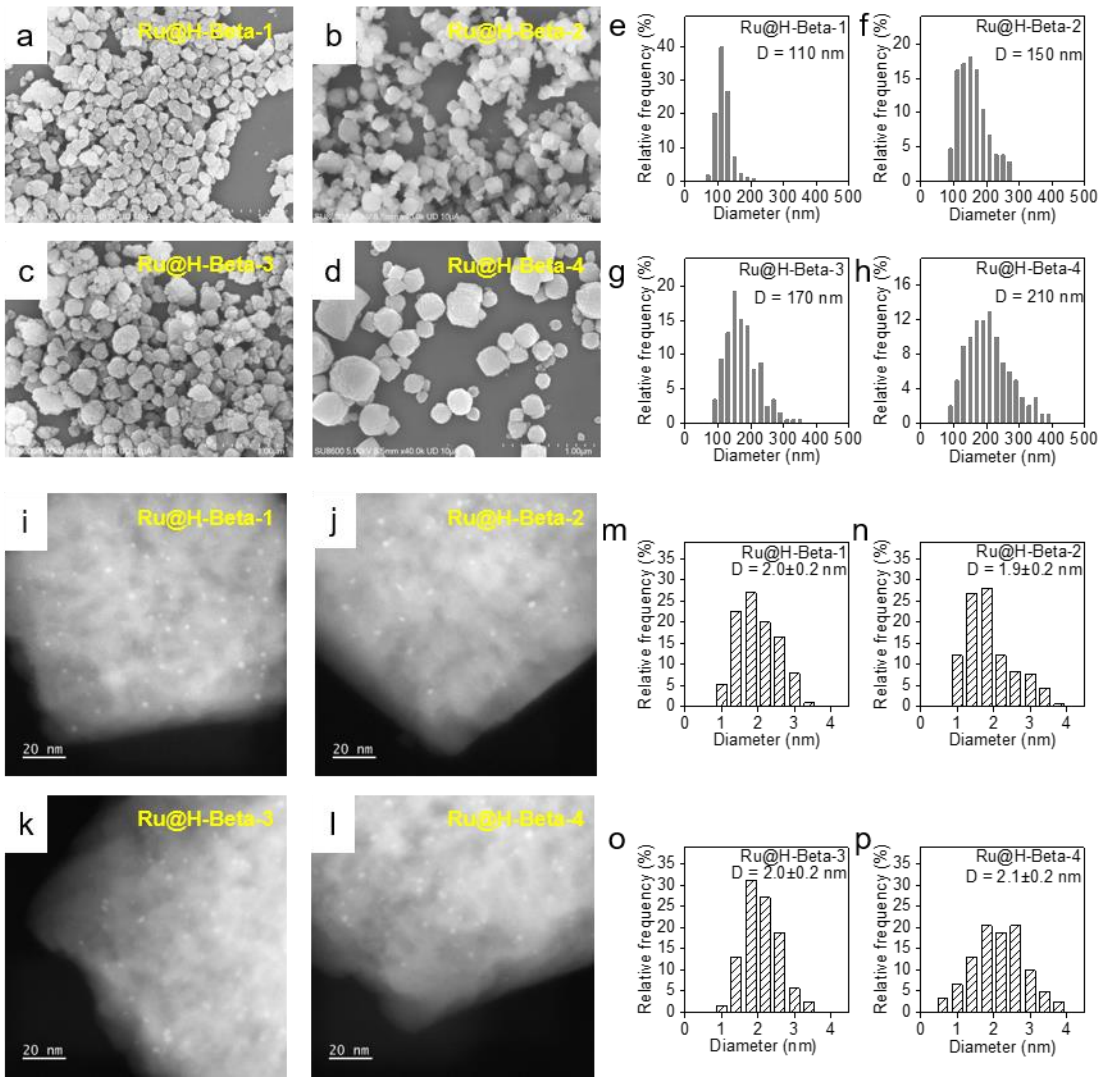

Supplementary Fig. 5. SEM and TEM images of Ru@H-Beta with varied H-Beta sizes. (a-d) SEM images. (e-h) The corresponding zeolite-particle size distributions. (i-l) TEM images. (m-p) The Ru particle size distributions in the corresponding samples. The H-Beta samples are named H-Beta-1 to H-Beta-4 in order of increasing the average zeolite-particle size.

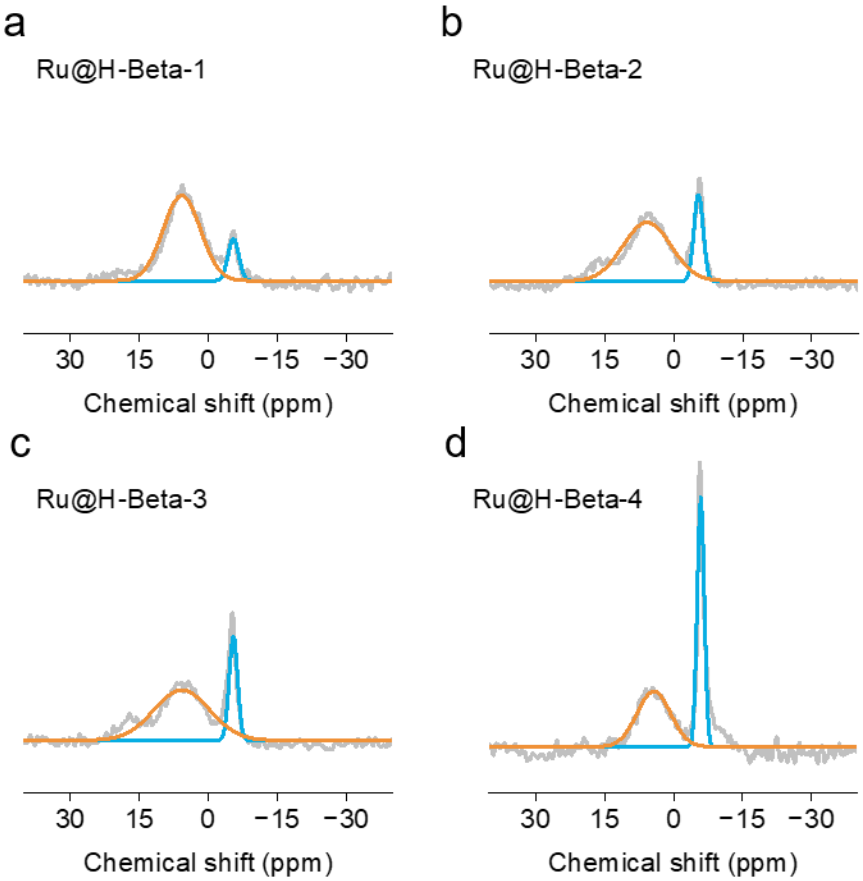

Supplementary Fig. 6. ^{31}P solid-state NMR spectra of Ru@H-Beta with varied H-Beta sizes. The H-Beta samples are named H-Beta-1 to H-Beta-4 in order of increasing the average zeolite-particle size, which can be found in Supplementary Fig. 5.

Triphenylphosphine (TPP), a base probe molecule with a kinetic diameter of 0.72 nm, is larger than the pore aperture of Beta zeolite (0.67 × 0.66 nm), and thus can selectively quantify the external acid sites[63]. The signal at δ (chemical shift) = 5.8 ppm corresponds to TPP adsorbed on the external Brønsted acid sites, while the peak at δ = −5.4 ppm arises from physisorbed TPP on the catalyst surface. The external Brønsted acid density was determined by integrating the δ = 5.8 ppm peak for each Ru@H-Beta sample. The calculated acid site density for each sample is summarized in Supplementary Table 6.

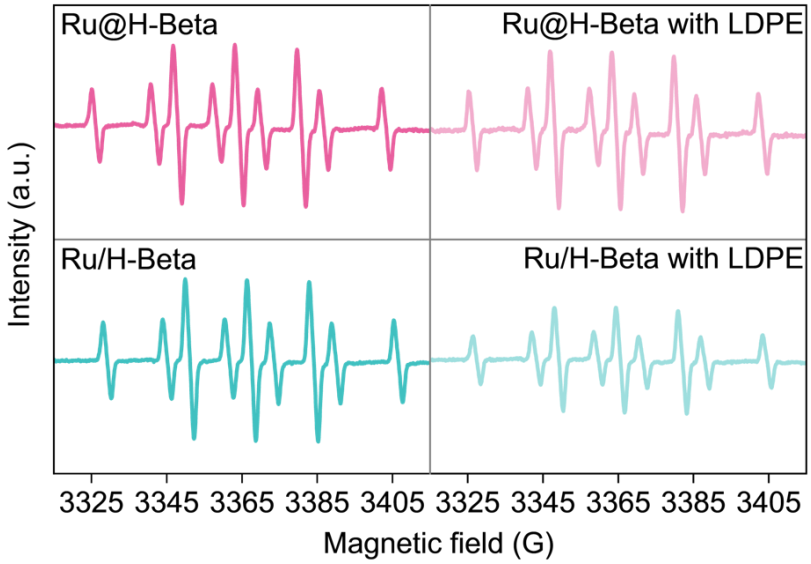

Supplementary Fig. 7. EPR spectra under H_2 using DMPO as a radical trap.

Ru@H-Beta and Ru/H-Beta show similar intensities for the H•–DMPO spin adduct under H_2 in the absence of LDPE (left). Upon blending with LDPE (LDPE/catalyst mass ratio = 1:3), the EPR signal intensity decreased remarkably for Ru/H-Beta, whereas that for Ru@H-Beta remained nearly unchanged. These results confirm that LDPE does not affect the formation of atomic hydrogen over Ru@H-Beta.

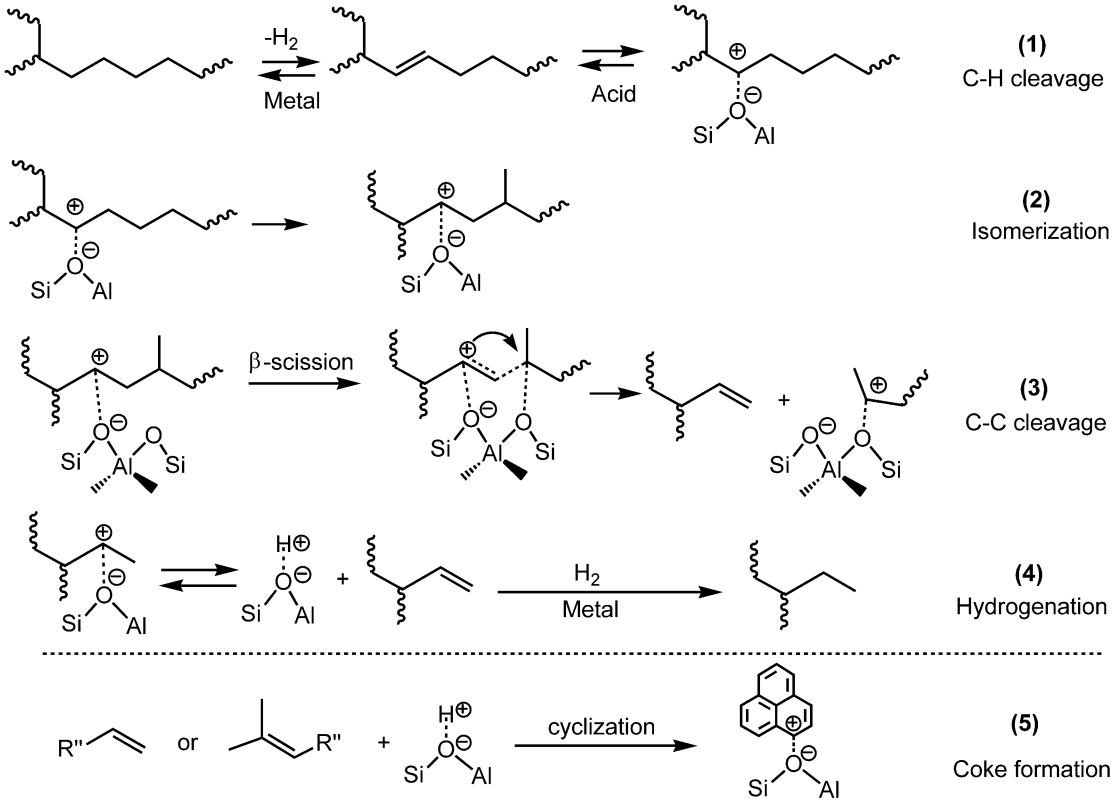

Supplementary Fig. 8. Proposed mechanism for LDPE conversion over zeolite-supported metal catalysts.

Ru/H-Beta represents a conventional metal/zeolite bifunctional catalyst. Over this type of catalyst, C−H bonds in LDPE are activated on metal sites, which can directly interact with the bulky LDPE polymer[17,18]. The resulting olefin, a dehydrogenation product, is subsequently protonated at an adjacent Brønsted acid site to form a carbenium ion (*Reaction 1*). This carbenium ion then undergoes isomerization and β-scission, cleaving the C−C bond at the β-position to yield a short-chain olefin and a shorter carbenium ion (*Reactions 2 and 3*). The shorter olefin is finally hydrogenated on metal sites to produce a shorter alkane, predominantly an isomer (*Reaction 4*). Repeated protonation, isomerization, and β-scission ultimately yield gasoline-range products.

Over Ru/H-Beta, the competitive co-adsorption of sticky LDPE and the formed olefins on Ru particles suppresses H_2 activation and olefin hydrogenation, thereby leading to coke formation (*Reaction 5*) and rapid catalyst deactivation.

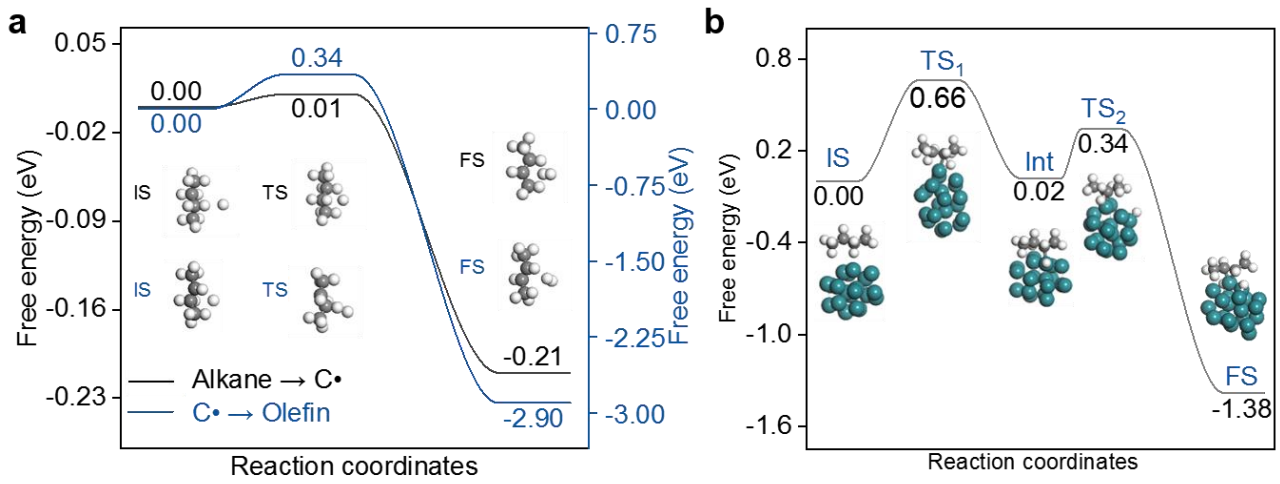

Supplementary Fig. 9. DFT calculations on free energies for alkane-to-olefin transformation. (a) Abstraction of H from alkane by hydrogen atoms. (b) Alkane activation on Ru clusters. Alkane: butane; IS: initial state; TS: transition state; FS: final state; Int: intermediate. Color code: grey, C; white, H; cyan, Ru. C• in (a) denotes carbon radical intermediate.

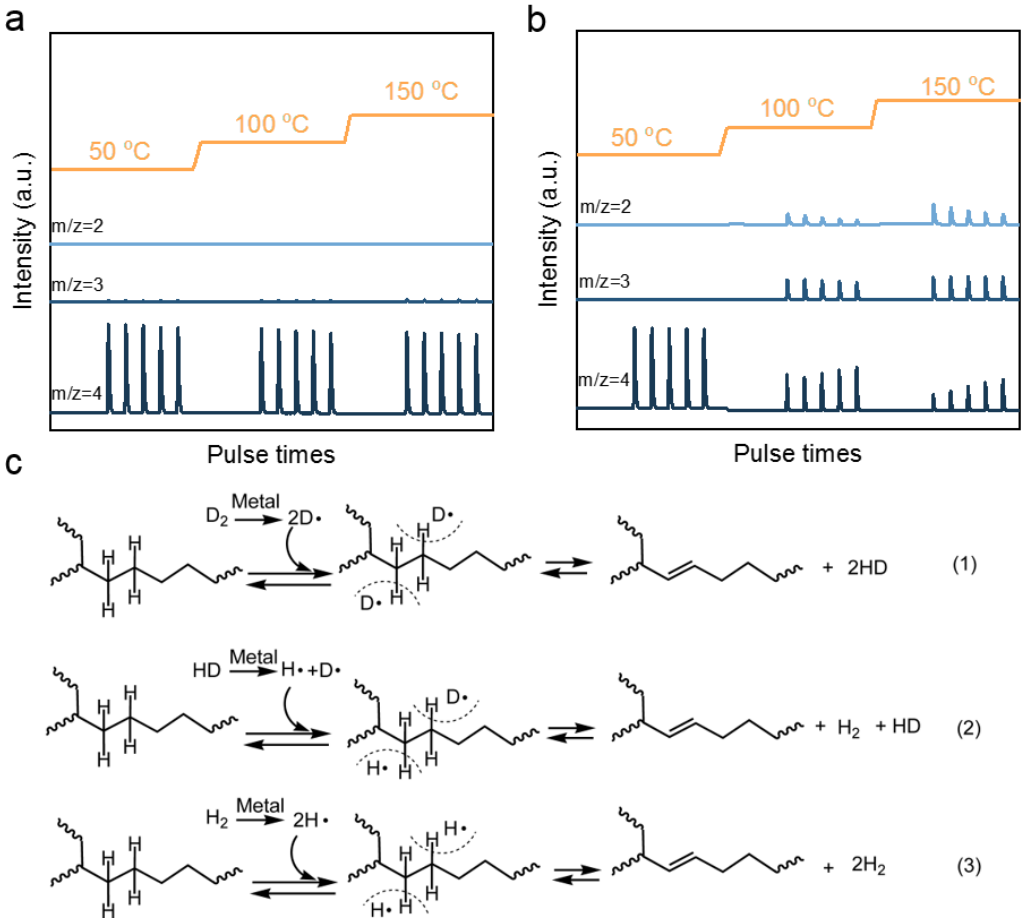

Supplementary Fig. 10. H/D exchange between D_2 and hydrogen in LDPE. (a) H-Beta + LDPE. (b) Ru@D-Beta + LDPE. (c) Possible H/D exchange mechanism. Experimental procedures: Ru@H-Beta was first converted to Ru@D-Beta to eliminate any interference from hydrogen originally present in the zeolite. This was achieved by treating Ru@H-Beta in a D_2 flow (20 mL min^{-1}) at 400 ºC for 3 hours. The resulting Ru@D-Beta was then physically mixed with LDPE at a mass ratio of 4:1. After purging with Ar at 50 ºC for 20 min, the mixture was maintained at the same temperature or at different temperatures (100 or 150 ºC). Multiple D_2 pulses were introduced, and the signals corresponding to H_2 (m/z = 2), HD (m/z = 3), and D_2 (m/z = 4) were monitored using a mass spectrometer.

Upon introducing D_2 pulses over the (Ru@D-Beta + LDPE) mixture at 50 ºC, neither H_2 nor HD was detected. However, when the temperature was raised to 100 and 150 ºC, the D_2 signal decreased, while signals corresponding to H_2 and HD emerged, indicating H/D exchange between hydrogen in LDPE and deuterium from D_2. In contrast, for the (H-Beta + LDPE) mixture, no formation of H_2 or HD was observed upon D_2 pulsing within the temperature range of 50–150 ºC. Given that the applied temperatures (50–150 ºC) are insufficient to crack LDPE and that no direct contact exists between LDPE and the encapsulated Ru sites in Ru@H-Beta, the detected HD must originate from the reaction between LDPE and D atoms generated *via* D_2 dissociation (*Reaction 1*). By the same mechanism, the resulting HD can further abstract hydrogen from LDPE, producing H_2 (*Reactions 2 and 3*). When Ru@D-Beta is replaced by H-Beta, the absence of metal sites prevents D_2 activation and subsequent hydrogen abstraction, thus accounting for the absence of both H_2 and HD signals.

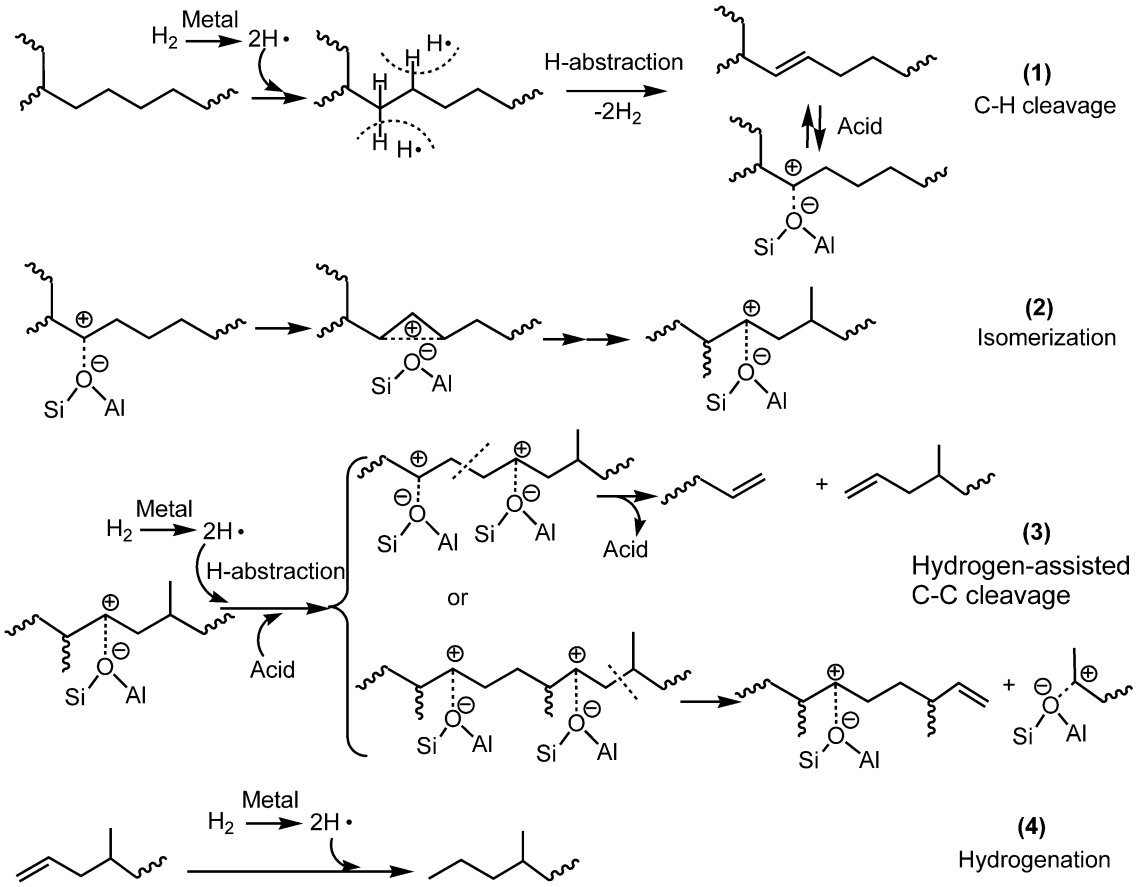

Supplementary Fig. 11. Proposed mechanism for LDPE conversion over metal@H-zeolite catalysts.

Although LDPE molecules cannot directly access the metal sites encapsulated within the zeolite, H_2 can be activated on these metals, and the resulting hydrogen atoms can migrate to the external surface. These hydrogen atoms promote the abstraction of hydrogen from C–H bonds in LDPE, leading to the formation of an olefinic intermediate (*Reaction 1*). This olefin is then protonated by an external Brønsted acid site to form a carbenium ion, which isomerizes into a branched carbenium ion (*Reaction 2*). The hydrogen atoms further facilitate additional H-abstraction events, generating multiple carbenium centers along the same polymer chain. Subsequent C–C bond cleavage of these carbenium ions produces a shorter olefin and new shorter-chain carbenium ions (*Reaction 3*). Finally, the shorter olefins are hydrogenated by atomic hydrogen that has migrated from the encapsulated metal sites (*Reaction 4*).

In the metal@H-zeolite catalyst, the encapsulation of metal sites within the zeolite prevents their blockage by sticky LDPE molecules or reaction intermediates. This architecture enables efficient H_2 activation and hydrogen spillover to the external surface, thereby promoting C–H bond activation and facilitating subsequent C–C cleavage. Furthermore, the active hydrogen species hydrogenate the resulting olefins, prompting their rapid desorption from acid sites. This mechanism not only prevents undesirable side reactions like cyclization and coking but also enhances the regeneration of acid sites.

Supplementary Table 1. Properties of H-Beta, Ru@H-Beta, and Ru/H-Beta.

Catalyst	Ru loadings[a] (%)	Ru particle size[b] (nm)	Si/Al ratio[c]	Brønsted acid density[d] (μmol g^{-1})	Specific surface area[e] (m^2 g^{-1})			Pore volume[e] (cm^3 g^{-1})
					S_{BET}	$S_{Internal}$	$S_{External}$	
H-Beta	-	-	12.5±0.1	663	562	412	150	0.21
Ru@H-Beta	0.23	2.0±0.2	12.3±0.2	638	609	430	179	0.22
Ru/H-Beta	0.26	2.1±0.2	12.1±0.2	651	600	445	155	0.23

[a] Calculated from ICP-MS.
[b] Estimated from TEM results.
[c] Calculated from XRF results.
[d] Calculated from NH_3-TPD results in Supplementary Fig. 1.
[e] Measured by N_2 physical adsorption.

Supplementary Table 2. Comparison of performance for LDPE upcycling under different reaction conditions.

LDPE weight (g)	Catalyst	Ru loading (%)	Catalyst weight (g)	*T* (°C)	*t* (h)	Conv. (%)	C_5–C_{12} yield (%)	C_5–C_{12} select. (%)	Formation rate of C_5–C_{12}	
									g g_{metal}^{-1} h^{-1}	g $g_{cat.}^{-1}$ h^{-1}
1.0	Ru@H-Beta	0.14	0.060	295	0.17	68	61	90	43713	61
1.0	Ru@H-Beta	0.14	0.060	275	0.5	100	90	90	21428	30
4.0	Ru@H-Beta	0.14	0.10	295	0.5	79	71	90	40571	57
5.0	Ru@H-Beta	0.14	0.30	275	0.5	100	88	88	20952	29
10	Ru@H-Beta	0.14	0.60	275	0.5	100	89	89	21190	30
150	Ru@H-Beta	0.23	8.0	275	1	100	86	86	7011	16
200	Ru@H-Beta	0.23	8.0	275	1.5	100	89	89	6449	15
1.0	Ru/H-Beta	0.26	0.060	275	0.5	43	31	88	3974	11

Supplementary Table 3. Comparison of performances of different catalytic systems for LDPE upcycling.

No.	LDPE weight (g)	Catalyst	Metal loading (%)	Cat. weight (g)	P_{H2} (MPa)	T (°C)	t (h)	C_5–C_{12} yield (%)	C_5–C_{12} select (%)	Formation rate of C_5–C_{12}[a]		Single-run metal usage[b] (g_{metal} ton_{LDPE}^{-1})	Ref.
										g g_{metal}^{-1} h^{-1}	g g_{cat}^{-1} h^{-1}		
1	1.0	Ru@H-Beta	0.07	0.060	3.0	275	1.0	89	89	21190	14.8	42	This work
	1.0	Ru@H-Beta	0.14	0.060	3.0	295	0.17	61	90	43713	61	124	
2	1.0	Ru/H-Beta	0.26	0.060	3.0	275	0.5	31	88	3974	10	420	This work
3	4.0	Ni/NbO*x*	1.0	0.20	3.0	260	5	70	70	280	2.8	500	*(64)*
4	1.4	Ru/C	5.0	0.050	2.2	225	16	45	45	16	0.79	1785	*(8)*
5	3.4	Ru/CeO_2	5.0	0.10	6.0	240	8	<83	<83	71	3.5	1470	*(65)*
6	2.0	Ru/WZr	5.0	0.050	5.0	250	2	15	28	60	3.0	2333	*(66)*
7	2.0	Pt/WZr	0.50	0.20	3.0	250	24	~90	~90	80	0.4	500	*(67)*
8	2.0	Pt/Ce-Y	4.9	0.20	3.0	300	2	81	81	83	4.1	4900	*(24)*
9	1.5	Ru/SBA-15	3.0	0.020	2.0	230	5	~27	~30	100	3.0	444	*(68)*
10	2.0	Pt/WO_3ZrO_2 &HY	0.25	0.20	3.0	250	2	72	72	1440	3.6	250	*(22)*
11	2.0	Pt@S-1 &HBeta	0.15	0.20	3.0	250	2	90	90	3000	4.5	150	*(23)*
12	4.0	Pt/USY-Cl	0.10	0.20	3.0	280	1	32	93	6882	6.9	145	*(25)*
13	5.0	Ru/HZSM-5	7.4	0.50	-[c]	280	24	<28	<40	1.6	0.12	10571	*(21)*
14	0.45	LSP-Z100	-[c]	0.090	-[c]	240	4	81	99	-[c]	1.0	-[c]	*(16)*
15	0.90	Ru/TiO_2	2.0	0.020	0.10	300	20	86	86	8.6	0.2	444	*(69)*
16	1.0	Pt/WO_3	0.20	0.10	3.0	250	3	77	77	1280	2.6	200	*(70)*
17	0.34	Ru_9Pt_{91}/C	21	0.020	0.50	300	24	~20	~20	16.2	3.4	12353	*(71)*
18	2.0	$NiMoS_x$/HY	-[c]	0.10	3.0	300	2	85	~90	-[c]	8.5	-[c]	*(72)*
19	2.0	Pt/HBeta	0.050	0.20	2.2	250	0.5	~56	~90	22400	11	80	*(26)*

[a] Calculations were based on metal amount or catalyst mass.

[b] Calculations were based on metal usage for the single-run conversion of LDPE.

[c] Not provided.

Supplementary Table 4. Catalytic transformations of different post-consumer plastic wastes.

Post-consumer plastic waste (main polymer)	Ru@H-Beta		Ru/H-Beta	
	Conv. (%)	C_5–C_{12} select. (%)	Conv. (%)	C_5–C_{12} select. (%)
Dropper (LDPE)	93	90	68	90
Sugar bottle (HDPE)	80	87	27	86
Cup (PP)	98	91	63	90
Cup lid (PS)	86	90	18	91
Coca-Cola bottle (PET)	88	PTA: >99%	63	PTA: >99%

Reaction conditions: post-consumer plastic waste, 1.0 g; catalyst, 0.060 g; 275 ºC; H_2, 3.0 MPa; 0.5 h for LDPE, HDPE and PP; 2 h for PS; 4 h for PET.

Supplementary Table 5. The atoms of LDPE models and Beta used for MD stimulations.

Different side chains on C_{20} ~ C_{2000} backbones						
Side chain / Backbone	None	$-CH_3$	$-C_2H_5$	$-C_3H_7$	$-C_4H_9$	$-C_5H_{11}$
C_{20}	$\{C_{20}H_{42}\}$*500	$\{C_{20}H_{40}(CH_3)_2\}$*500	$\{C_{20}H_{40}(C_2H_5)_2\}$*500	$\{C_{20}H_{40}(C_3H_7)_2\}$*500	$\{C_{20}H_{40}(C_4H_9)_2\}$*500	$\{C_{20}H_{40}(C_5H_{11})_2\}$*500
C_{100}	$\{C_{100}H_{202}\}$*100	$\{C_{100}H_{200}(CH_3)_2\}$*100	$\{C_{100}H_{200}(C_2H_5)_2\}$*100	$\{C_{100}H_{200}(C_3H_7)_2\}$*100	$\{C_{100}H_{200}(C_4H_9)_2\}$*100	$\{C_{100}H_{200}(C_5H_{11})_2\}$*100
C_{200}	$\{C_{200}H_{402}\}$*50	$\{C_{200}H_{399}(CH_3)_3\}$*50	$\{C_{200}H_{399}(C_2H_5)_3\}$*50	$\{C_{200}H_{399}(C_3H_7)_3\}$*50	$\{C_{200}H_{399}(C_4H_9)_3\}$*50	$\{C_{200}H_{399}(C_5H_{11})_3\}$*50
C_{500}	$\{C_{500}H_{1002}\}$*20	$\{C_{500}H_{996}(CH_3)_6\}$*20	$\{C_{500}H_{996}(C_2H_5)_6\}$*20	$\{C_{500}H_{996}(C_3H_7)_6\}$*20	$\{C_{500}H_{996}(C_4H_9)_6\}$*20	$\{C_{500}H_{996}(C_5H_{11})_6\}$*20
C_{1000}	$\{C_{1000}H_{2002}\}$*10	$\{C_{1000}H_{1991}CH_3)_{11}\}$*10	$\{C_{1000}H_{1991}C_2H_5)_{11}\}$*10	$\{C_{1000}H_{1991}C_3H_7)_{11}\}$*10	$\{C_{1000}H_{1991}C_4H_9)_{11}\}$*10	$\{C_{1000}H_{1991}C_5H_{11})_{11}\}$*10
C_{2000}	$\{C_{2000}H_{4002}\}$*5	$\{C_{2000}H_{3981}(CH_3)_{21}\}$*5	$\{C_{2000}H_{3981}(C_2H_5)_{21}\}$*5	$\{C_{2000}H_{3981}(C_3H_7)_{21}\}$*5	$\{C_{2000}H_{3981}(C_4H_9)_{21}\}$*5	$\{C_{2000}H_{3981}(C_5H_{11})_{21}\}$*5
Beta zeolite						
Unit cell length (a*b*c)			Total number of atoms			
79*76*80			21168			

Polyethylene model structures are defined by the notation $\{C_{x1}H_{y1}(C_{x2}H_{y2})_n\}$*N, where:
$C_{x1}H_{y1}$: The carbon backbone structure.
x_1,y_1: Number of carbon and hydrogen atoms in the carbon backbones.
$C_{x2}H_{y2}$: A branched segment (side chain).
x_2,y_2: Number of carbon and hydrogen atoms in a branch.
n: Number of branches attached to the carbon backbones.
N: Number of carbon backbones.

Supplementary Table 6. Properties and catalytic performance of Ru@H-Beta with different zeolite crystallite sizes.

Catalyst	Ru particle diameter[a] (nm)	Zeolite crystallite size[b] (nm)	*t*-Plot external surface area[c] (m^2 g^{-1})	Total Brønsted acid density[d] (μmol g^{-1})	External surface Brønsted acid density[e] (μmol g^{-1})	LDPE Conv.[f] (%)
Ru@H-Beta-1	2.0±0.2	110	179	638	135	79
Ru@H-Beta-2	1.9±0.2	150	168	681	120	73
Ru@H-Beta-3	2.0±0.2	170	151	616	117	68
Ru@H-Beta-4	2.1±0.2	210	107	678	80	40

[a] Estimated from TEM results in Supplementary Fig. 5.

[b] Estimated from SEM results in Supplementary Fig. 5.

[c] Measured by N_2 physical adsorption.

[d] Calculated from NH_3-TPD results.

[e] Calculated from ^{31}P SSNMR data in Supplementary Fig. 6.

[f] Reaction conditions for LDPE conversion: LDPE, 1.0 g; catalyst, 0.060 g; H_2, 3.0 MPa; 275 ºC; 20 min.